Nonribosomal peptide synthetase gene clusters and characteristics of predicted NRPS-dependent siderophore synthetases in *Armillaria* and other species in the Physalacriaceae

Deborah L. Narh Mensah[1,2], Brenda D. Wingfield[1] & Martin P. A. Coetzee [1,*]

[1]Departments of Biochemistry, Genetics and Microbiology, Forestry and Agricultural Biotechnology Institute (FABI), Faculty of Natural and Agricultural Sciences, University of Pretoria, Pretoria, South Africa

[2]Council for Scientific and Industrial Research-Food Research Institute (CSIR-FRI), P. O. Box M20, Accra, Ghana

*Correspondence to Martin P. A. Coetzee. Email: martin.coetzee@fabi.up.ac.za

Abstract

Fungal secondary metabolites are often pathogenicity or virulence factors synthesized by genes contained in secondary metabolite gene clusters (SMGCs). Nonribosomal polypeptide synthetase (NRPS) clusters are SMGCs which produce peptides such as siderophores, the high affinity ferric iron chelating compounds required for iron uptake under aerobic conditions. *Armillaria* spp. are mostly facultative necrotrophs of woody plants. NRPS-dependent siderophore synthetase (NDSS) clusters of *Armillaria* spp. and selected Physalacriaceae were investigated using a comparative genomics approach. Siderophore biosynthesis by strains of selected *Armillaria* spp. was evaluated using CAS and split-CAS assays. At least one NRPS cluster and other clusters were detected in the genomes studied. No correlation was observed between the number and types of SMGCs and reported pathogenicity of the species studied. The genomes contained one NDSS cluster each. All NDSSs were multi-modular with the domain architecture $(ATC)_3(TC)_2$. NDSS clusters of the *Armillaria* spp. showed a high degree of microsynteny. In the genomes of *Desarmillaria* spp. and *Guyanagaster necrorhizus,* NDSS clusters were more syntenic with NDSS clusters of *Armillaria* spp. than to those of the other Physalacriaceae species studied. Three A-domain orthologous groups were identified in the NDSSs, and atypical Stachelhaus codes were predicted for the A3 orthologous group. In vitro biosynthesis of mainly hydroxamate and some catecholate siderophores was observed. Hence, *Armillaria* spp. generally contain one highly conserved, NDSS cluster although some interspecific variations in the products of these clusters is expected. Results from this study lays the groundwork for future studies to elucidate the molecular biology of fungal phyto-pathogenicity.

Keywords: Basidiomycetes; Comparative genomics; Iron acquisition; Phytopathogenic fungi; Secondary metabolism; Siderophore

Introduction

Microorganisms, including fungi, are known to produce diverse low molecular weight organic compounds known as secondary metabolites (SMs). Microbial SMs typically mediate ecological interactions such as mutualism (Amin et al. 2009; Johnson et al. 2013), competition (Butaitė et al. 2017; Stubbendieck and Straight 2016), predation (Stubbendieck and Straight 2016) and pathogenicity (Oide et al. 2006), and play a critical role in microbial survival in

ecological niches (Kuo et al. 2020; Stubbendieck and Straight 2016). These metabolites include terpenes or terpenoids (e.g., Melleolides) (Engels et al. 2011; König et al. 2019), polyketides (PKSs; e.g., Lovastatin) (Amnuaykanjanasin et al. 2005; Gunde-Cimerman and Cimerman 1995), and Nonribosomal peptides (NRPs; e.g., epidithiodioxopiperazines and siderophores) (Brandenburger et al. 2017; Eisendle et al. 2003; Kuo et al. 2020; Le Govic et al. 2019; Schwecke et al. 2006; Welzel et al. 2005; Winterberg et al. 2010; Yuan et al. 2001). Genes involved in fungal SMs biosynthesis are located in secondary metabolite gene clusters (SMGCs) which contain genes that encode biosynthetic enzymes such as terpene cyclases, polyketide synthases, and Nonribosomal peptide synthetases (NRPSs), usually named according to the SM types they produce (Brandenburger et al. 2017; Kadi and Challis 2009; Le Govic et al. 2018, 2019).

NRPSs are multifunctional enzymes which assemble the SM backbone structure by use of multiple active sites known as domains. The adenylation (A), thiolation (T; also known as peptide carrier protein, PCP), and condensation (C) domains are required for NRPS functionality. Other domains, classified as accessory domains, such as epimerization (E), formylation (F), methylation (M), reduction (R), oxidation (Ox), and thioesterase (TE) are optional and confer some structural and functional differences to the NRPs synthesized. A-domains are responsible for substrate selection and activation using ATP, whereas T- and C-domains catalyze phosphopantetheine (PP)-linkages of substrates with thioester bonds and peptide- or ester-bond formation between two adjacent linked substrates, respectively (Kadi and Challis 2009; Walsh 2008). TE domains often terminate NRP synthesis, although reductive chain termination is sometimes employed in the synthesis (Kadi and Challis 2009). NRPS are described as either monomodular if they contain only one set of the main domains or multi-modular when they contain more than one complete set of domains and may contain accessory domains (Kadi and Challis 2009; Le Govic et al. 2019). The multiplicity of the modules in an NRPS as well as the number and types of accessory domains it contains influence the complexity and structural diversity of the peptides synthesized (Gaitatzis et al. 2001).

Other enzymes in NRPS clusters function in glycosylation, acylation, halogenation, or hydroxylation for modifying the NRPS substrate or the NRP synthesized, and regulation for regulating production of the NRP (Brandenburger et al. 2017; Le Govic et al. 2018, 2019). NRPS clusters may also include transporters for transporting the synthesized peptide. Other enzymes in the NRPS clusters include monooxygenases, acyltransferases, major facilitator transporters, and Zn_2Cys_6 transcription factor (Brandenburger et al. 2017; Le Govic et al. 2018, 2019). Genes encoding these proteins have been reported in NRPS-dependent siderophore synthetase (NDSS) clusters (Brandenburger et al. 2017; Le Govic et al. 2018, 2019).

Siderophores are peptides biosynthesized using one of the two main biosynthesis pathways. These are the NRPS-dependent siderophore synthetase pathway or the NRPS-independent siderophore (NIS) synthetase pathway (Brandenburger et al. 2017; Iftime et al. 2016; Kadi and Challis 2009; Kurth et al. 2016; Salwan and Sharma 2020). A third pathway, called the hybrid NRPS/NIS pathway, which utilizes a blend of both pathways may also be used (Kadi and Challis 2009; Salwan and Sharma 2020).

Siderophores are used by fungi (Brandenburger et al. 2017; Chen et al. 2019; Johnson et al. 2013; Koulman et al. 2012; Kuo et al. 2020; Mukherjee et al. 2018; Narh Mensah et al. 2018; Schrettl et al. 2007; Wallner et al. 2009; Welzel et al. 2005; Yuan et al. 2001;) and other organisms (Audenaert et al. 2002; Butaitė et al. 2017; Carrano et al. 2001; Devireddy et al. 2010; Kügler et al. 2020; Maglangit et al. 2019; Schrettl et al. 2007; Taguchi et al. 2010; Wang

et al. 2021;) to solubilize, sequester, transport/shuttle, and store ferric iron (Fe^{3+}) especially under iron-limiting conditions, such as aerobic conditions (Schrettl et al. 2007). Siderophores are also involved in other biological functions such as structuring microbial communities and, in the case of pathogenic siderophore producers, enhancing virulence factors and suppression of host defense mechanisms (Amin et al. 2009; Gu et al. 2020; Paauw et al. 2009; Taguchi et al. 2010). Based on the structure of their Fe^{3+}-chelating functional groups, these molecules are grouped into five classes; catecholates and phenolates (collectively called aryl caps), hydroxamate, carboxylates, and mixed type, which have at least two Fe^{3+}-coordinating moieties (Carrano et al. 2001; Haas et al. 2008).

Fungal siderophores have been implicated in outcompeting or inhibition of plant pathogens, alteration of host defense mechanisms such as induced systemic resistance, as well as alteration of plant-fungal interactions (Johnson et al. 2013; Mukherjee et al. 2018). The intracellular siderophores ferricrocin and hydroxyferricrocin have been reported being required for germ tube formation, asexual sporulation, resistance to oxidative stress, catalase A activity, and virulence in *Aspergillus fumigatus* (Schrettl et al. 2007). The plant endophytic fungus, *Epichloë festucae,* produces the extracellular siderophore epichloënin A (Johnson et al. 2013). This siderophore is believed to serve as an important molecular/cellular signal for controlling fungal growth (Johnson et al. 2013). Lack of epichloënin A can alter the homeostasis of the symbiotic relationship between *E. festucae* and its host, *Lolium perenne,* from being mutually beneficial to being antagonistic (Johnson et al. 2013). *Trichoderma* spp., including *T. virens*, produce siderophores that suppress growth of *Armillaria* spp. when they are grown together in cultures (Chen et al. 2019).

Armillaria spp. are terrestrial ubiquitous white-rot basidiomycetes in the family Physalacriaceae, and typically have a broad host range (Baumgartner and Rizzo 2002; Coetzee et al. 2003; Elías-Román et al. 2018; Prospero et al. 2004; Warwell et al. 2019). *Desarmillaria* spp., that were previously treated as *Armillaria* spp., are exannulate species which include *Desarmillaria tabescens* and *D. ectypa* (Koch et al. 2017). Fungi in these genera have mycorrhizal, saprophytic, and/or pathogenic symbiotic relationships with plants and most of the species are considered to be facultative necrotrophs (Baumgartner and Rizzo 2002; Coetzee et al. 2003; Elías-Román et al. 2018; Prospero et al. 2004; Warwell et al. 2019). Other members of the Physalacriaceae that were considered in the current study include the closely related *Guyanagaster necrorhizus,* that shares a recent ancestor with *Armillaria* (Koch et al. 2017), as well as *Cylindrobasidium torrendii* and *Oudemansiella mucida*. Studies aiming to understand and eventually inhibit the predominantly pathogenic *Armillaria* species and the adverse effects they have on horticulture, agriculture, and forestry are therefore warranted.

In this study, we hypothesize that variation in siderophore production by various species and strains of *Armillaria* may influence the reported pathogenicity of these fungi. To test this hypothesis, we investigated the genomes of selected *Armillaria* spp. and other members of the Physalacriaceae to identify the types and numbers of SMGCs in the genomes in silico. We also determined the presence and putative characteristics of NRPS-dependent siderophore biosynthesis clusters in the genomes. Finally, we characterized the NRPS-dependent siderophore biosynthesis genes in comparison to those characterized in other organisms in silico. We also utilized bioassays to evaluate the production and the types of siderophores produced by strains representing selected *Armillaria* spp.

Materials and methods

All in silico studies were performed according to the flowchart presented in Fig. S1. For in vitro studies, all glassware was washed with 6 M HCl followed by 3 washes with doubly deionized H_2O (ddH_2O) to remove all trace metals before use (Schwyn and Neilands 1987). Media were autoclaved at 121 °C for 20 min.

In silico identification of secondary metabolite gene clusters

Genome mining of selected strains

Whole genomes of *Armillaria* spp. and other members of the Physalacriaceae (Table 1) were mined for SMGCs using previously described methods (Agger et al. 2009; Le Govic et al. 2019; Sayari et al. 2019) but with some modification. In brief, secondary metabolite gene clusters in each of the genomes under study were predicted with the Antibiotics & Secondary Metabolite Analysis SHell (antiSMASH) using the fungal version (fungiSMASH) v. 6.0.0alpha1-56f63c8 (Blin et al. 2019a). Genome sequences uploaded into fungiSMASH for these analyses were initially annotated, with gene annotation files obtained from the Mycocosm fungal genome sequence database of JGI (https://mycocosm.jgi.doe.gov/mycocosm/home/releases?flt=Physalacriaceae) in CLC Main Workbench v21.0.4 (www.qiagenbioinformatics.com) using the "Annotate with GFF/GTF/GVF file" plugin. Relaxed detection strictness was used for these analyses. All extra features (excluding the Cluster-border prediction based on transcription factor binding sites (CASSIS) feature, which was inactive during the study) were also activated. Cluster boundaries were manually delimited up to approximately 10 Kb upstream and 30 Kb downstream of the cluster boundaries detected by fungiSMASH. These regions were selected to account for the large non-coding region in the *A. novae-zelandiae* cluster. Minimum Information about a Biosynthetic Gene (MIBiG) cluster comparison, ClusterBlast, KnownClusterBlast, Cluster Pfam Analysis, and Pfam-based GO term annotation were used for the purpose of detecting similar gene clusters. All of these are implemented in fungiSMASH. MIBiG comparison shows areas that are similar to the region of the query biosynthetic gene cluster (BGC) in the MIBiG Database (Blin et al. 2019b; Medema et al. 2015). ClusterBlast recovers gene clusters from the antiSMASH database and other clusters of interest that are homologous to the query gene cluster (Medema et al. 2011). KnownClusterBlast shows clusters from the MIBiG database that are similar to the current region (Blin et al. 2019a). Various types of secondary metabolite clusters were identified in the analyzed genomes by fungiSMASH. However, since the focus of this study was on NRPS-dependent siderophore synthetase (NDSS) clusters, all further analyses were conducted only on predicted NDSS clusters.

Gene annotation, gene order confirmation, and generation of cluster synteny maps

The gene order and orientation were predicted using results obtained from fungiSMASH and the genome annotations obtained using CLC Main Workbench. Putative gene annotation was done by conducting a tBLASTn search using the amino acid sequences of the respective genes (as obtained from fungiSMASH) in the NCBI BLAST web-based tool using default parameters (https://blast.ncbi.nlm.nih.gov/Blast.cgi). The search parameter was altered to include only Fungi (taxid:4751) for all the NRPS gene sequences because the sequences were longer than 4000 amino acids. The top 100 closest orthologs obtained were sorted according to percentage identity and the closest experimentally characterized orthologs were used for the putative annotation of the identified genes in the clusters. All other genes in the flanking regions beyond

Table 1 Genome features of studied Physalacriaceae

Species	Strain	Code	Ploidy	Length (Mb)	# of genes	Genome source[a]
Armillaria borealis	FPL87.14	Armbor1	–	71.69	19,984	JGI
Armillaria cepistipes	B5	Armcep1	Haploid	75.50	23,460	JGI (Sipos et al. 2017)
Armillaria fumosa	CBS 122,221	Armfum1	–	55.82	16,095	JGI
Armillaria mellea	ELDO17	Armme1	–	70.86	15,646	JGI
Armillaria nabsnona	CMW6904	Armnabs1	Haploid	62.72	19,015	JGI
Armillaria novae-zelandiae	2840	Armnov1	Diploid	79.33	18,551	JGI
Desarmillaria ectypa	FPL83.16	(Des)Armect1	–	40.60	12,228	JGI
Desarmillaria tabescens	CCBAS 213	(Des)Armtab1	–	74.88	19,032	JGI
Cylindrobasidium torrendii	FP15055 v1.0	Cylto1	Haploid	31.57	13,940	JGI (Floudas et al. 2015)
Guyanagaster necrorhizus	MCA 3950 v1.0	Guyne1	–	53.69	14,276	JGI and GenBank (accession: JAEACO000000000.1) (Koch et al. 2021)
Oudemansiella mucida	CBS 558.79 v1.0	Oudmuc1	–	61.73	18,562	JGI (Ruiz-Dueñas et al. 2021)

[a]All genomes citing JGI without a reference or made public after November 2018 were used with permission from Dr. László G. Nagy

NB All the studied genomes had RNA sequences available (JGI and respective references)

the cluster boundaries predicted by fungiSMASH were annotated by conducting tBLASTx searches with the annotated sequences using the BLAST tool implemented in CLC Main Workbench against the NCBI database. Other information for the flanking genes were obtained from InterProScan. Cluster synteny maps were drawn using EasyFig v2.2.5 (Sullivan et al. 2011).

In silico characterization of NRPS-dependent siderophore synthetases

Determination of size, intron number, domain architecture and modular organization of NRPSs

Number of introns of predicted NDSS genes were observed in CLC based on the annotated genomes described in "Genome mining of selected strains" which include the use of RNAseq data. Size information of these genes were obtained from fungiSMASH. The size of the amino acid sequence was confirmed with InterProScan (https://www.ebi.ac.uk/interpro/). The domain architectures and modular organizations of identified NDSS were obtained from fungiSMASH, as well as Pfam searches in InterProScan using the amino acid sequences. Any disparities observed between the data from the two approaches were reconciled with results obtained from searches of the amino acid sequence of the respective gene against the Pfam v 33.1 web-based tool (https://pfam.xfam.org/). Attempts to use the PKS/NRPS Analysis Website (http://nrps.igs.umaryland.edu/) (Bachmann and Ravel 2009), was not successful as most of the domains were not recognized by the tool.

A-domain phylogenetic analyses and substrate specificity prediction

Datasets of the amino acid sequences of the A-domains of the NDSSs identified in the Physalacriaceae (obtained from fungiSMASH) were combined with the A-domain amino acid sequences of experimentally characterized NDSSs from other species, which had relatively high similarity (based on the results of the BLAST searches conducted under "Gene annotation, gene order confirmation, and generation of cluster synteny maps" to the putative NDSS genes of the presently studied members of the Physalacriaceae. The amino acid sequence of the A3 domain of *A. novae-zelandiae* was obtained from the region identified from Pfam analysis. Sequences were aligned using the MUSCLE algorithm in the MEGA X software (Stecher et al. 2020). Maximum likelihood algorithm implemented in MEGA X with the LG substitution model was used to construct a phylogenetic tree. Nodal support was obtained using 100 bootstrap replications and with the same setting used to obtain the phylogenetic tree.

NDSS A-domain specificities (i.e., amino acid codes and substrate specificities) were predicted using NRPSpredictor2 (Rausch et al. 2005; Röttig et al. 2011) implemented in fungiSMASH. NRPSpredictor2 uses both the signature sequence method (Stachelhaus codes or amino acid codes) (Stachelhaus et al. 1999) and the Support Vector Machines (SVM)-based method (Rausch et al. 2005; Röttig et al. 2011). The predicted A-domain specificities were compared to those of other characterized NDSSs which were found to be orthologous to the NDSSs identified in the present study.

Table 2 *Armillaria* spp. lifestyle, culture codes and source information

Species	Lifestyle[a]	CMW number	Host	Original source
A. fuscipes	Facultative necrotroph/ pathogenic	CMW2740	*Pinus elliottii*	Entabeni, South Africa
		CMW3164	*Pelargonium asperum*	La Réunion
A. gallica	Facultative necrotroph/ weakly pathogenic	CMW31092	N/A	Veneto, Bellune, Italy
		CMW45397	Duff	Minnesota, USA
A. luteobubalina	Facultative necrotroph/ pathogenic	CMW4974	N/A	Australia
A. mellea	Facultative necrotroph/ highly pathogenic	CMW31132	*Ailanthus altissima*	China
A. nabsnona	Weakly pathogenic	CMW3159	*Acer macrophyllum*	Vancouver, Canada
		CMW6904	*Acer circinatum*	USA
Armillaria sp. ACB	N/A	CMW4456	*Brachystegia utilis*	Stapleford, Zimbabwe

ACB African Clade B in Coetzee et al. (2005), *N/A* Not available

[a]Lifestyle information are summarized from Koch et al. (2017)

Assessment of siderophore production potential of selected *Armillaria* strains

Fungal strains, maintenance, and growth conditions

The fungal cultures used were strains of *A. fuscipes, A. gallica, A. mellea, A. luteobubalina* and *A. nabsnona* (Table 2). These species were selected to represent *Armillaria* species reported to have different ecology in terms of pathogenicity and virulence, and to serve as a proof-of-concept for siderophore biosynthesis by *Armillaria* species. Cultures were maintained on malt yeast extract agar (MYA) medium (15 g/L malt extract, 2 g/L yeast extract, 15 g/L agar) and incubated at 25 ± 2 °C in the dark for 53 days. All reagents were purchased from commercial suppliers.

Siderophore detection

Siderophore production and activity was detected by both the universal chrome azurol S agar (CAS) (Alexander and Zuberer 1991) and the modified chrome azurol S agar medium (split CAS/MYA) (Milagres et al. 1999) assays. These methods were used to detect siderophore production as well as generally characterize the siderophores produced by the mycelia and rhizomorphs of the studied strains of *Armillaria* species. CAS agar at pH 6.8 was prepared using the method described by Alexander and Zuberer (1991). Plates were dried overnight in a flow cabinet to ensure excess water was removed and incubation of strains followed the description above. Three replicates for each strain on each media were used in this study.

Split CAS/MYA plates were prepared as follows. CAS agar medium and MYA were separately prepared, sterilized and maintained at 50 °C in a water bath. MYA was poured first in the petri dishes and allowed to set for 1 h. Half of the set MYA was aseptically cut and discarded, followed by pouring the cooled CAS media into the empty half of the plate and allowing to set. The experiment was also performed using only MYA media to investigate differences, if any, in mycelia and rhizomorph growth rates on the CAS media in comparison to the growth media.

Cultures were inoculated in the center of the CAS and MYA plates, and in the middle of the MYA part of the split CAS/MYA plates. The inoculum consisted of 1 cm^2 culture discs sub-cultured from an actively growing strain on MYA medium. Plates were observed for change of the CAS media from blue to reddish-orange, orange, purplish-red, and purple (Arora and Verma 2017; Milagres et al. 1999). The type of siderophore produced was classified according to the color change. Mycelia macro-morphology was observed directly as judged by the investigators to detect any effect of culture media on culture morphology. Un-inoculated plates served as the control for this experiment.

Results

Identification of secondary metabolite biosynthesis gene clusters

Secondary metabolite gene clusters in the studied Physalacriaceae genomes

Different secondary metabolite gene clusters putatively determined as being involved in various secondary metabolite biosynthesis were identified in the genomes of the species included in this study using in silico analyses (Fig. 1). These SMGCs included NRPS, NRPS-like, siderophores (suspected NIS clusters), type 1 polyketide synthases (T1PKS), terpenes, as well as hybrid clusters including NRPS-Like/Terpene, NRPS-Like/T1 PKS, and

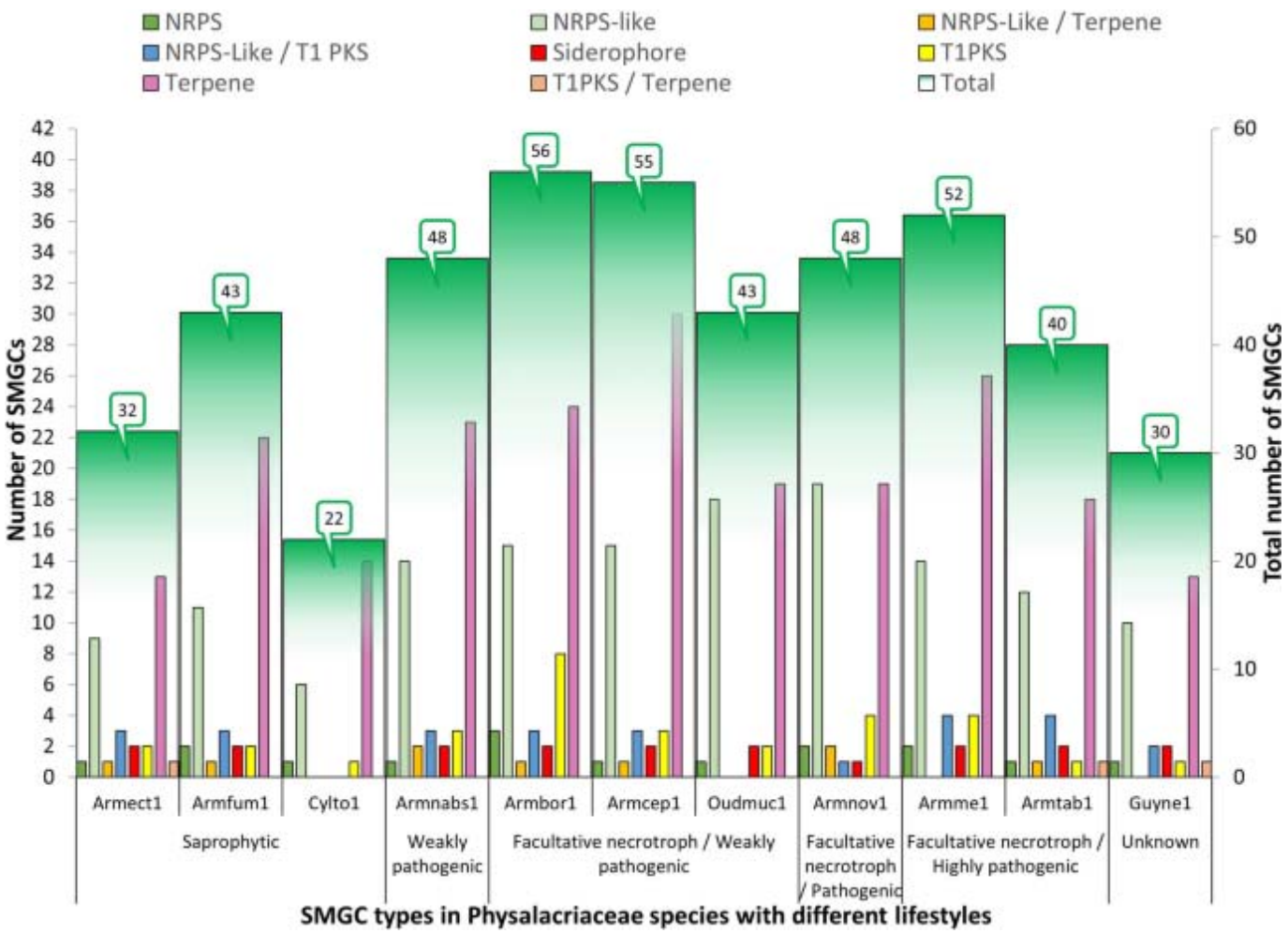

Fig. 1. SMGC diversity and distribution in genomes of the studied *Armillaria* spp. and other Physalacriaceae with different lifestyles. Different classes or types of SMGCs, as predicted by fungiSMASH are presented by different colors. NRPS = Nonribosomal polypeptide synthetase, T1PKS = Type1 polyketide synthetase, Siderophores = suspected NIS synthetase clusters. NRPS-Like / Terpene, NRPS-Like / T1PKS, T1PKS/Terpene are predicted hybrid clusters. All genomes studied contained at least 22 SMGCs that may produce diverse compounds. Oudmuc1 contained 1 SMGC predicted to produce indole (Data not shown). Lifestyle information are summarized from Koch et al. (2017)

T1PKS/Terpene clusters. The genome of *O. mucida* also contained a cluster predicted to be involved in the production of indole (data not shown).

The total number of SMGCs in the *Armillaria* and *Desarmillaria* genomes ranged from 32 in *D. tabescens* to 56 in *A. borealis* (Fig. 1). The most abundant type of gene clusters in the genomes were the terpenes (13–30 clusters), followed by NRPS-like (9–19 clusters), and T1PKS (1–8 clusters). The maximum number of NPRS, siderophore, and hybrid clusters detected were 3, 3, and 5, respectively. *Cylindrobasidium torrendii* was unique for possessing only 4 types of secondary metabolite clusters, totaling 22 in its genome (14 terpenes, 6 NRPS-like, and 1 each of NRPS and T1PKS).

No direct correlation was observed between the number and types of SMGCs and reported pathogenicity (Fig. 1). For instance, the pathogenic species, *A. novae-zelandiae* contained 48 (1 NRPS, 19 terpenes, 4 T1PKS) SMGCs. Likewise, the relatively weakly pathogenic species, *A. nabsnona* also contained 48 SMGCs (1 NRPS, 23 terpenes, 3 T1PKS). The facultative necrotrophs which are weakly pathogenic, *A. borealis* and *A. cepistipes*, contained a total of 56 (3 NRPS, 24 terpenes, 8 T1PKS) and 55 (1 NRPS, 30 terpenes, 3 T1PKS) SMGCs, respectively. The closely related species, *G. necrorhizus* contained a total of 30 SMGCs (1 NRPS, 13 terpene, 1 T1PKS). The pathogenicity of this species is unknown.

In all the genomes studied, the NRPS gene in only one of the different NRPS clusters identified by fungiSMASH in each species showed hits in the MIBiG database. The hit with the strongest support for all species (% identity = 27.0, % coverage = 107.1, BLAST score = 1438.0, *E* value = 0.0) was with the epichloenin_A_synthetase cluster (accession number AET13875.1, which produces an extracellular siderophore identified in *Epichloë festucae*). There was no hit for the ClusterBlast nor KnownClusterBlast. All further analysis was conducted on this cluster since NRPS-dependent siderophore synthetase clusters was the focus of this study.

Gene annotation and synteny comparison of NRPS-dependent siderophore synthetase clusters and flanking genes

Genome walking of the regions up- and downstream of the clusters identified by fungiSMASH (Table S1) revealed that the predicted NDSS clusters in the *Armillaria* and *Desarmillaria* species studied ranged from approximately 72 Kb in *A. fumosa* to approximately 100 Kb in *A. novae-zelandiae*. The clusters identified in the other members of the Physalacriaceae were approximately 67, 51, and 94 Kb in *C. torrendii*, *G. necrorhizus*, and *O. mucida,* respectively.

The NDSS clusters in the *Armillaria* and *Desarmillaria* species were largely syntenic (Fig. 2, Table S2). However, the NDSS genes of *A. mellea* and *D. ectypa* showed less conserved synteny. The flanking genes located upstream of the NDSS genes contained a syntenic block comprising genes that encode RecF/RecN/SMC (involved in structural maintenance of chromosomes), choline/ethanolaminephospho-transferase, cellobiose dehydrogenase and at least one Major Facilitator Superfamily transporter (MFS) gene. The upstream region also contained genes encoding (membrane-bound) hypothetical proteins and natterin-like hypothetical proteins. These genes and the intergenic regions also showed a high degree of synteny. The genes downstream of the NDSS genes were generally syntenic for most species of *Armillaria* and *Desarmillaria* although an inversion was observed in *A. borealis* (Fig. 2). *A. mellea* was unique for possessing cytochrome P450 genes downstream of the NDSS gene. The species in the phylogenetic sister genus of *Armillaria*, *D. ectypa* and *D. tabescens,* had unique genes downstream of the NDSS genes. The genes putatively encode a member of the

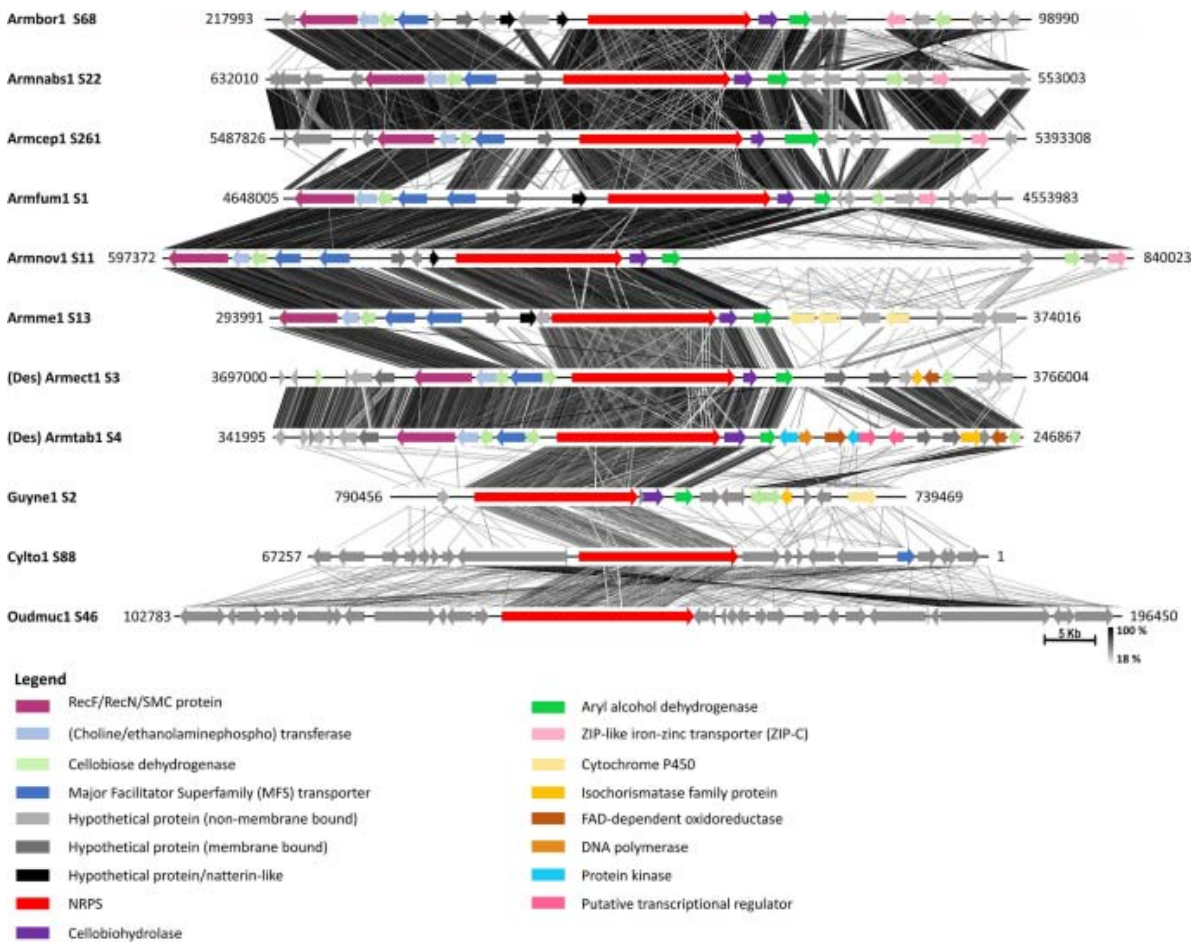

Fig. 2. NDSS gene cluster synteny map in annotated genomes of Physalacriaceae. Numbers following the species code are the scaffolds on which the clusters are located. Different colors and orientation of arrows represent different putative proteins as determined by tBLASTn searches and direction of transcription respectively. Orthologous genes are identically colored. All genes colored gray in the clusters of Cylto1 and Oudmuc1 are not orthologous to the genes in the clusters of the other members of the Physalacriaceae. Darker shades of lines between clusters represent higher amino acid similarity between the different clusters based on tBLASTx. Numbers at the ends of the clusters are the locations on the scaffolds

Isochorismatase family protein, FAD-dependent oxidoreductase, cellobiose dehydrogenase, as well as (membrane-bound) hypothetical proteins (Fig. 2, Table S2). These genes were not found when a search was conducted further downstream of the cluster for the *Armillaria* species. In addition to these genes, a DNA polymerase gene as well as two copies each of protein kinase and putative transcriptional regulator genes were uniquely found in the NDSS gene cluster in *D. tabescens*. Genes flanking the NDSS genes of *C. torrendii* and *O. mucida* included cytochrome C oxidase, Zn_2Cys_6 fungal-type domain-containing protein, alpha/beta-hydrolase, or mannitol dehydrogenase, and various (membrane-bound) hypothetical or uncharacterized proteins (data not shown).

Characteristics of identified NRPSs

Size, intron number, domain architecture and modular organization of NRPSs

The size in base pairs (bp) of the NDSS genes ranged from 15,689 in *C. torrendii* (Cylto1_490369) to 19,023 in *O. mucida* (Oudmuc1_1435297) (Table 3). The smallest and largest size of the translated amino acids in these genes was found in Armbor1_1740653 (4329 aa) and Oudmuc1_1435297 (5353 aa), respectively. The number of introns in the NRPS genes ranged from 45 in Cylto1_490369 to 58 in Oudmuc1_1435297 (Table 3). The protein sequences of the NDSS genes showed significant matches (query cover 80–97%; percentage identity 26.5–34.5%; expected value 0.0) with translated nucleotide sequences of characterized NDSS genes in different fungi responsible for hydroxamate ferricrocin-type siderophore biosynthesis, as well as the uncharacterized *NRPS2* in *W. ichthyophaga* EXF-994 (Table 3). The NDSSs were all multi-modular showing three complete A-T-C modules organization ending with two T-C didomains [$(A\text{-}T\text{-}C)_3(T\text{-}C)_2$] (Table 4). Guyne1_959764, as well as the NDSSs of *As. fischeri* and *F. sacchari,* also contained a C-terminal of an A-domain after the first A-domain.

Table 3 Gene characteristics of putative NRPS-dependent siderophore synthetase of studied Physalacriaceae genomes and similarity to characterized NRPS-dependent siderophore synthases

ProteinID[a]	Location in genome[b]	Strand	Size[c]	# of introns	Query cover and Percentage identity[d] (%)				
					Fer3 (4830 aa) *Ustilago maydis*	FSN1 (4707 aa) *Fusarium sacchari*	NRPS2 (4339 aa) *Wallemia ichthyophaga*	SidC (4759 aa) *Aspergillus fischeri*	SidN (4690 aa) *Epichloë festucae*
Armbor1_1740653	cds153656_169842 (68.1)	–	16,186 (4329)	52	95 (31.2)	96 (34.5)	95 (41.6)	96 (31.5)	94 (26.5)
Armcep1_12756	cds5429960_5446141 (261.7)	–	16,181 (4530)	50	96 (29.5)	97 (32.6)	96 (42.9)	97 (33.5)	95 (28.3)
Armfum1_1505943	cds4583838_4599965 (1.5)	–	16,126 (4521)	50	97 (29)	97 (31.7)	96 (42.2)	96 (32.9)	96 (26.8)
Armme1_963312	cds326940_343118 (13.1)	+	16,177 (4533)	50	96 (29.9)	97 (32.5)	96 (42.6)	96 (33.4)	95 (28.2)
Armnabs1_1027822	cds577121_593305 (22.1)	–	16,183 (4539)	50	96 (29.7)	97 (32.5)	96 (42.9)	97 (33.4)	95 (28.2)
Armnov1_1625296	cds756488_772706 (11.1)	+	16,217 (4244)	57	82 (31.3)	83 (33.1)	88 (44.3)	88 (34)	81 (27.9)
(Des) Armect1_1380706	cds3727079_3743248 (3.1)	+	16,168 (4533)	50	96 (29.3)	96 (32.5)	95 (42.3)	95 (33.1)	95 (28.2)
(Des) Armtab1_1636500	cds293769_309930 (4.1)	–	16,160 (4551)	49	96 (29.7)	96 (32.7)	96 (42.6)	96 (33.3)	95 (28.6)
Cylto1_490369	cds24790_40480 (88.1)	–	15,689 (4485)	45	95 (29.8)	95 (32.3)	95 (40.5)	95 (33.2)	97 (28.5)
Guyne1_959764	cds765973_782126 (2.1)	–	16,152 (4527)	50	97 (30)	97 (32.3)	96 (42.1)	97 (32.8)	96 (28.1)
Oudmuc1_1435297	cds135154_154178 (46.1)	+	19,023 (5353)	58	81 (30.1)	81 (32.6)	80 (41.3)	81 (33.6)	80 (28.8)

[a]Genome code followed by ProteinId from JGI

[b]Presented as coding sequence number (Scaffold number followed by the Secondary metabolite cluster number located on the scaffold, after the decimal point, as determined by fungiSMASH)

[c]Presented as number of base pairs (bp) of DNA sequence (number of amino acids (aa) in translated protein sequence)

[d]Matches of FerrichromeA synthetase (Fer3), Ferrirhodin synthetase (FSN1), Nonribosomal peptide synthetase 2 (NRPS2), Ferricrocin synthetase (SidC), and Epichloënin A synthetase (SidN) with accession numbers XM_011389001.1, JN997437.1, XM_009271380.1, XM_001264036.1, and JN132403.1 respectively, obtained from tBLASTn analyses. The species within which proteins are found are indicated. Sizes of the respective proteins are presented in brackets and the organisms in which the proteins are reported are placed below the codes. The NRPS2 protein has not been characterized but is the closest match (in terms of percentage identity) in all the genomes studied. Data presented as Query cover (Percentage identity)

Table 4 Comparison of modular organization of NRPS genes of Physalacriaceae to NRPS genes of other fungi

Protein ID [a]	Modular organization [b]		Reference(s)
	fungiSMASH	InterProScan and Pfam	
Armbor1_1740653	A T C A T C A T C T C T C	A T C A T C A T C T C T C	This study
Armcep1_12756	A C A T C A T C T C T C	A T C A T C A T C T C T C	This study
Armfum1_1505943	A T C A T C A T C T C T C	A T C A T C A T C T C T C	This study
Armme1_963312	A T C A T C A T C T C T C	A T C A T C A T C T C T C	This study
Armnabs1_1027822	A T C A T C A T C T C T C	A T C A T C A T C T C T C	This study
Armnov1_1625296	A C A T C T C T C T C	A T C A T C A T C T C T C	This study
(Des)Armect1_1380706	A T C A C A T C T C T C	A T C A T C A T C T C T C	This study
(Des)Armtab1_1636500	A T C A T C A T C T C T C	A T C A T C A T C T C T C	This study
Cylto1_490369	A T C A T C A T C T C T C	A T C A T C A T C T C T C	This study
Guyne1_959764	A C A T C A T C T C T C	A A T C A T C A T C T C T C	This study
Oudmuc1_1435297	A C A T C A C T C T C	A T C A T C A T C T C T C	This study
EAW22140 (SidC)	N/A	A A T C A T C A T C T C T C	This study
EAL91050 (SidC)	N/A	A T C A T C A T C T C T C	Schwecke et al. (2006)
AAP56239 (SidC)	N/A	A T C A T C A T C T C T C	Schwecke et al. (2006)
AET13875.1 (SidN)	N/A	A T C A T C A T C T C T C	Johnson et al. (2007), This study
AET13879.1 (SidN)	N/A	A T C A T C A T C T C T C	Johnson et al. (2007), This study
AFD36451.1 (FSN1)	N/A	A A T C A T C A T C T C T C	Munawar et al. (2013), This study
AAX49356.1 (Fso1)	N/A	A T C A T C A T C T C T C	(Schwecke et al., 2006; Welzel et al., 2005)
KIS71541.1 (Fer3)	N/A	A T C A T C A T C T C T C	(Schwecke et al., 2006; Winterberg et al., 2010), This study
EOQ99429.1 (NRPS2)	N/A	A T C A T C A T C T C T C	This study

[a]Protein identity for *Armillaria* spp. and other Physalacriaceae species. NCBI accession numbers for protein sequences of NRPS of other species are provided. The names of the genes are placed in brackets. EAL91050, AAP56239, AET13875.1, AFD36451.1, AAX49356.1, and KIS71541.1 are found within the genomes of *As. fumigatus* Af293, *As. nidulans*, *E. festucae* strain E2368, *F. sacchari*, *Om. olearius*, and *U. maydis* 521, respectively. These proteins synthesize the siderophores, Ferricrocin, Ferricrocin, Epichloënin A, Ferrirhodin, Ferrichrome A, and Ferrichrome A, respectively. The secondary metabolites synthesized by EAW22140 of *As. fischeri* NRRL 181, AET13879.1 of *E. festucae* strain F11, and EOQ99429.1 of *W. ichthyophaga* EXF-994, have not yet been characterized.

[b]Modular organization is domain architecture based on fungiSMASH and Pfam searches for all Physalacriaceae species and on Pfam searches for all other NRPSs. A = adenylation domain (also known as AMP-binding enzyme), T = thiolation domain (also known as Phosphopantetheine attachment site; PCP), C = condensation domain. For fungiSMASH-based modular organization, all blank spaces indicate absence of a domain. For InterProScan and Pfam-based modular organization, all domains marked by solid fill with white font color, and solid fill with black font color had significant and insignificant matches in the Pfam database, respectively. Domains marked with texture fill with black font color were AMP-binding enzyme C-terminal domain. All the NRPS fall under the Type II structural type according to the classification system described by Schwecke et al. (2006). N/A = not applicable

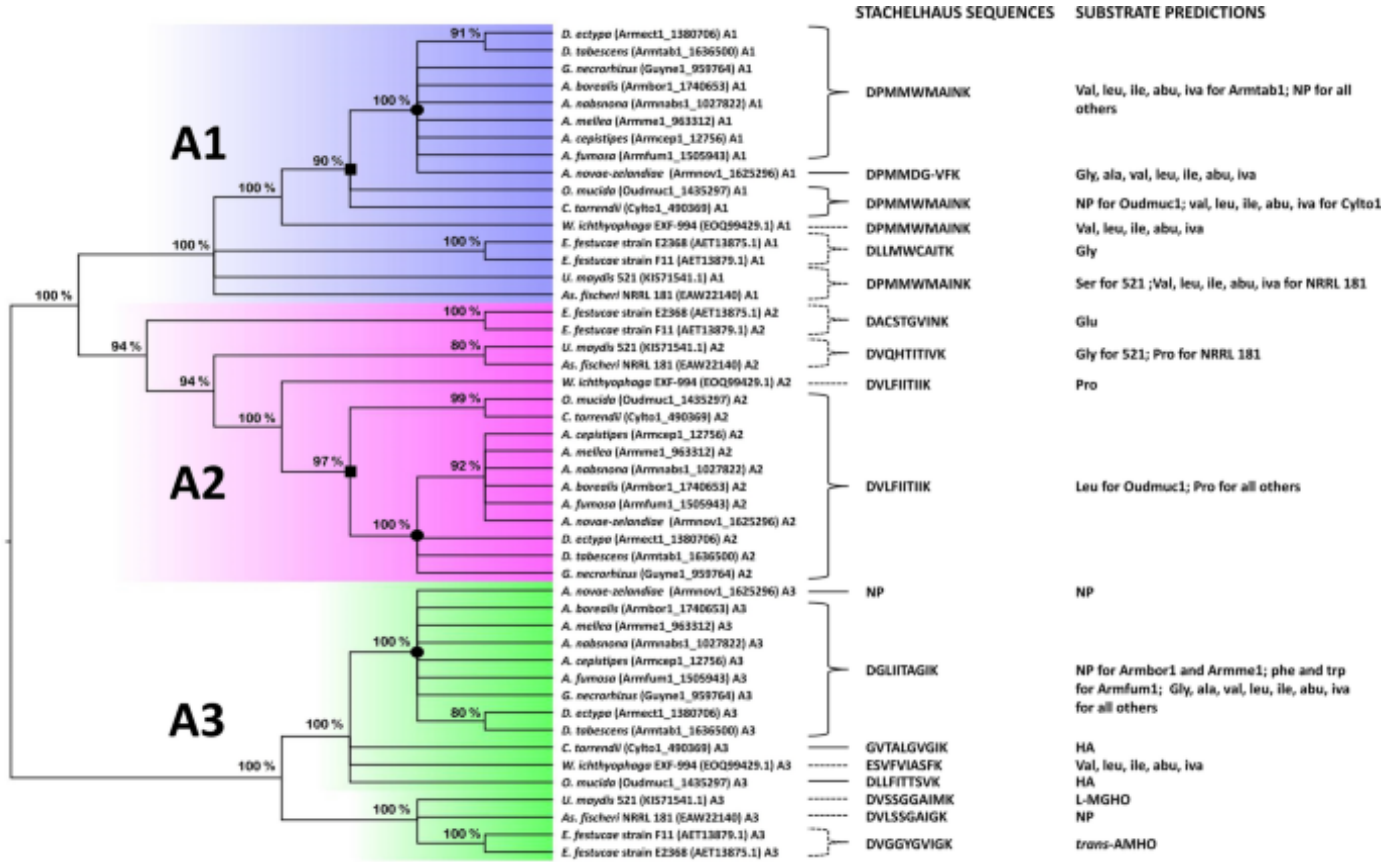

Fig. 3. Phylogenetic tree and substrate predictions of A1–A3 domains of putative NDSSs in *Armillaria* and other Physalacriaceae genomes in comparison with *NRPS2* of *W. ichthyophaga* and other characterized NDSSs in other fungi. Bootstrap support values greater than 70% are shown above each node. Species names of putative NDSSs in *Armillaria* and other Physalacriaceae genomes are shown followed by ProteinIDs in brackets and the A-domain numbers. All other NDSSs are presented as species (and strain) followed by NCBI accession numbers in bracket and the A-domain numbers. Colored areas are A1, A2, and A3 domains of NDSSs respectively. Nodes marked with black squares highlight the nodes which group the Physalacriaceae. Nodes marked with black ovals highlight the *Armillaria* spp., *Desarmillaria* spp. and *G. necrorhizus* clade of each A-domain. Solid brackets and lines refer to Physalacriaceae species. Dashes refer to other fungal species. All Stachelhaus sequences and (predicted) substrates of all characterized NRPS-dependent siderophore synthetases from other fungi except that of *As. fischeri* NRRL 181 were obtained from various authors (Johnson et al. 2007; Schwecke et al. 2006; Welzel et al. 2005; Winterberg et al. 2010). NP = None predicted, HA = hydrophobic-aliphatic amino acids, L-MGO = N^5-*trans*-(α-methyl)-glutaconyl-N^5-hydroxy-L-ornithine, and *trans*-AMHO = N^5-*trans*-anhydromevalonyl-N^5-hydroxyornithine

Phylogeny, Stachelhaus sequences, and substrate specificity of A-domains of putative NDSSs

Phylogenetic analysis of the A1–A3 domains of the putative NDSSs placed the sequences in three main clusters with strong nodal support in the phylogenetic tree (Fig. 3). These clusters represented the different domains A1, A2 and A3, respectively. All A1 domains formed a sister group with the A2-domain cluster with 97% bootstrap support. The A3-domain cluster formed a sister group to the A1 and A2 clusters. Within the A1 and A2-domain clusters, sequences from species in the Physalacriaceae formed respective monophyletic groups.

Sequences of all *Armillaria* species, except for those from *A. novae-zelandiae*, formed supported monophyletic groups within the A1 and A3-domain clusters. In the A1 domain cluster, the sequence of *A. novae-zelandiae* was more closely related to that of *G. necrorhizus*, a species that is in the sister genus of *Armillaria* and *Desarmillaria*. Within the A2-domain cluster, sequences from all *Armillaria* species formed a strongly supported group. In all three domain clusters, sequences from *D. ectypa* and *D. tabescens* formed groups separated from the *Armillaria* species but phylogenetically more closely related to species of *Armillaria* than to those of other Physalacriaceae. In all three domain clusters, sequences of *G. necrorhizus* were placed more closely related to *Armillaria* and *Desarmillaria* than to sequences from other species in the Physalacriaceae.

Stachelhaus codes and predicted substrate specificities for the A-domains of the predicted NDSSs of the members of the Physalacriaceae in comparison to those reported for characterized NDSSs in other fungal species gave more insights about the characteristics of the presently studied NDSSs (Fig. 3). The code of the A1 domains of the studied species was in most cases DPMMWMAINK. Those for *A. novae-zelandiae* (Armnov1_1625296), *E. festucae* strain E2368, and *E. festucae* strain F11 were DPMMDG-VFK, DLLMWCAITK, and DLLMWCAITK, respectively (Fig. 3). The code of the A2 domains of all the studied members of the Physalacriaceae were the same (DVLFIITIIK). This code was shared with the A2 domain of the NRPS of the halophilic basidiomycete, *W. ichthyophaga* EXF-994. In contrast, the A2-domain code of the basidiomycete, *U. maydis* 521 was DVQHTITVVK (Schwecke et al. 2006; Winterberg et al. 2010). A different A2-domain code (DVQHTITIVK) was shared by the ascomycetes, *As. fischeri* and *As. fumigatus* (Schwecke et al. 2006). Among these fungi, *As. nudilans* differed in that it contained a valine (val) instead of an isoleucine (iso) at the 8th position of the A2-domain code, although both amino acids have hydrophobic side chains. The A3 domains were more diverse. *C. torrendii* (Cylto1_490369) had the distinct A3-domain code, GVTALGVGIK, which only shared the last three amino acids of the A3-domain code of the *Armillaria* and *Desarmillaria* species. *O. mucida* (Oudmuc1_1435297) also had a unique A3-domain code, ESVFVIASFK.

<u>Siderophore production and mycelia growth of selected Armillaria spp.</u>

Siderophores were produced by all the strains studied in both the CAS and CAS/MYA media (Fig. 4). The CAS media on some of the plates (e.g., *A. fuscipes* strains CMW2740 and CMW3164, and *A. mellea* strain CMW31132 on CAS) showed different discoloration from blue to orange and/or reddish-orange closer to the mycelia to purple and/or purplish-red further from the mycelia and rhizomorphs, indicative of co-production of different types of (extracellular) siderophores by the strains studied. This was also the case for *A. luteobubalina* strain CMW4974 and *A. nabsnona* strain CMW6904 on CAS/MYA. The change of CAS media

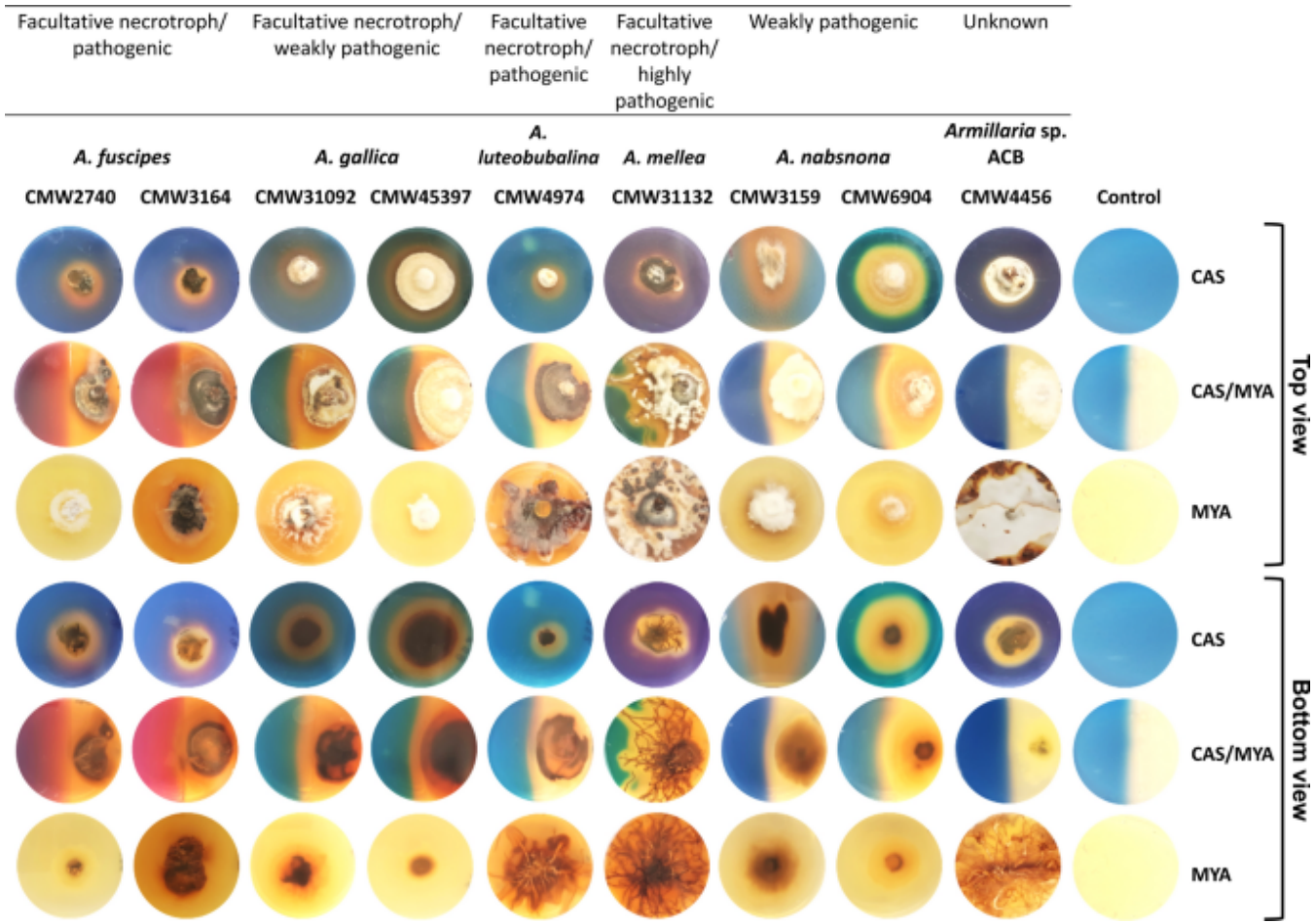

Fig. 4. Representative plates showing siderophore biosynthesis and mycelia and rhizomorph growth of various species and strains of *Armillaria.* Top and bottom views of representative plates of *Armillaria* spp. on CAS, CAS/MYA, and MYA on 45th day of incubation. Note the color change of the blue CAS media to purplish-red (e.g., CMW3164 on CAS/MYA), purple (e.g., CMW4456 on CAS), reddish-orange (e.g., CMW3159 on CAS), and/or orange (e.g., CMW6904 on CAS) mostly beyond the margins of the mycelia and/or rhizomorphs indicative of production of different types of (extracellular) siderophores. Control plates are the respective uninoculated media. ACB = African Clade B

from blue to purplish-red for *A. fuscipes* strains CMW2740 and CMW3164 was notably more pronounced on CAS/MYA than on CAS.

Mycelia culture morphology and growth rates were altered on the CAS media for some cultures (Fig. 4). For instance, growth rate of *A. luteobubalina* strain CMW4974 was fastest on MYA followed by CAS/MYA and slowest on CAS by the end of the incubation period. The reverse trend was observed for *A. nabsnona* strain CMW6904 that showed the fastest culture growth on CAS and slowest growth on MYA. *Armillaria luteobubalina* strain CMW4974 changed from crustose mycelia on MYA to cottony mycelia on CAS. Both mycelia and rhizomorph growth of *A. luteobubalina* strain CMW4974 and *Armillaria* sp. ACB strain CMW4456 were slower when cultured on CAS and CAS/MYA compared to MYA.

Discussion

Genome-wide identification of secondary metabolite gene clusters

Secondary metabolite gene clusters in the studied genomes

In this study we explored the diversity of secondary metabolite gene clusters in the genomes of *Armillaria* spp., *Desarmillaria* spp. and other members of the Physalacriaceae using a variety of bioinformatic tools. Different types of SMGCs namely NRPS, T1PKS, NRPS-Like and Terpene, as well as hybrid clusters NRPS-Like/T1PKS, NRPS-Like/Terpene T1PKS/Terpene were identified in the genomes. Clusters identified to be responsible for siderophore biosynthesis (suspected NRPS-independent siderophore biosynthesis clusters) by fungiSMASH were also identified in the genomes of the fungi studied. These types of SMGCs ranged in their numbers among the fungi.

There was no correlation in terms of cluster number and fungal lifestyle. Although this was unexpected, we postulate that the role of the secondary metabolites/metabolism in the studied species in relation to pathogenicity and/or virulence will be influenced by various biotic and abiotic factors such as the specific host and its state during host-fungal interaction, competing organisms in the environment, pH, temperature, and nutrient availability in the environment, and molecular factors such as transcription factors and other regulators. This assertion is supported by the fact that pathogenicity and/or virulence of *Armillaria* spp. and strains are in themselves affected by various factors such as intra species variation, forest management systems, host species, state of the hosts (e.g., stressed or healthy), as well as environmental factors (e.g., elevation) (Legrand et al. 1996; Mesanza et al. 2017; Prospero et al. 2004; Tsykun et al. 2012). The factors influencing the regulation and role of (plant-pathogenic) fungal SMs has been reviewed by various authors including Macheleidt et al. (2016) and Pusztahelyi et al. (2015).

The results of this research agree with previous studies on secondary metabolite genes and gene clusters in *Armillaria* species. Sipos et al. (2017) showed that 5 trichodiene genes, 1 polyprenyl synthase gene, and 6 polyketide synthase genes are expressed in the rhizomorphs of *Armillaria* spp. Engels et al. (2011) have reported on genes and gene clusters responsible for the biosynthesis of melleolides and armillyl orsellinates in *A. gallica*. In addition, various polyketides synthesized by polyketide synthases in PKS clusters have been reported to be produced by fungi (Gunde-Cimerman and Cimerman 1995). These include lovastatin identified in a white-rot basidiomycete species belonging to the genus *Pleurotus* (Gunde-Cimerman and Cimerman 1995), as well as depudecin and 19,20-epoxycytochalasin Q synthesized by the

woody plant saprophytic or weakly pathogenic ascomycete species in the genus *Xylaria* (Amnuaykanjanasin et al. 2005). The low (less than 50%) identities of the best hits in characterized NRPS gene clusters in MIBiG database, and the absence of hits for ClusterBlast and KnownClusterBlast, suggests novelty of these NRPS gene clusters detected in the Physalacriaceae. A hit of less than 50% in the MIBiG database was used to predict the novelty of thumolycin biosynthetic gene clusters in *Bacillus thuringiensis* (Zheng et al. 2018).

Synteny of predicted NDSS gene clusters and neighboring genes

The predicted NDSS gene clusters and the neighboring genes showed a high degree of microsynteny both among the genes and the intergenic regions despite the observed inversion and duplication events in some of the clusters. However, there were some variations in the cluster for *A. mellea, A. novae-zelandiae, D. ectypa*, and *D. tabescens.* Conserved synteny/similarity in biosynthetic gene clusters among species from the same genera has previously been reported and this is also reflected in this study (Evdokias et al. 2021; Goering et al. 2016).

Compared to the *Armillaria* spp., the genes downstream from the Aryl-alcohol dehydrogenase genes differed in the *Desarmillaria* spp. *Desarmillaria tabescens* harbored a unique set of genes that included a gene which encodes an isochorismatase family protein. An ortholog of this gene was also found in the predicted NDSS gene cluster of *G. necrorhizus*. An isochorismatase and an isochorismate synthase gene have been reported to be located within an NDSS gene cluster of *Streptomyces* sp. strain ATCC 700,974 (Patzer and Braun 2010). This cluster synthesizes the catechol-peptide siderophore, griseobactin (Patzer and Braun 2010). Additionally, a bifunctional isochorismate lyase/aryl carrier protein, DhbB, has been identified in an NRPS-dependent catecholic siderophore biosynthesis operon of *Bacillus subtilis*, which synthesizes itoic acid (2,3-dihydroxybenzoate (DHB)-glycine) (May et al. 2001).

Genes typical of those in NDSS gene clusters were identified in this study. These included monooxygenases, dehydrogenases, oxidoreductases, transferases, transporters, and transcription factors (Eisendle et al. 2003; Schwecke et al. 2006; Welzel et al. 2005; Winterberg et al. 2010). Contrary to our findings, the NRPS cluster in *S. apiospermum* contains an L-ornithine-N^5-monooxygenase gene just downstream of the NRPS gene, SAPIO_CDS9032. L-ornithine-N^5-monooxygenase genes have also been reported in the NDSS clusters of the ascomycetes, *Schizosaccharomyces pombe* (Schwecke et al. 2006), *As. fumigatus* (Schrettl et al. 2007), and *As. nudilans* (Eisendle et al. 2003), as well as the basidiomycetes, *C. subvermispora* (Brandenburger et al. 2017), *Omphalotus olearius* (Welzel et al. 2005), and *Ustilago maydis* (Winterberg et al. 2010). This enzyme catalyzes N^5-hydroxylation of L-ornithine during hydroxamate-type siderophore biosynthesis (Eisendle et al. 2003). The absence of the L-ornithine-N^5-monooxygenase genes in the presently studied NDSS gene clusters indicates that the products of the latter will be structurally different from those of the characterized clusters in other fungi. This assertion is also supported by the absence of a hit in the ClusterBlast and KnownClusterBlast searches.

NDSS gene characteristics

Genetic and structural characteristics of identified NDSS genes

The characteristics of the identified NDSS genes were largely similar among the *Armillaria* and *Desarmillaria* spp. in comparison to other members of the Physalacriaceae and the

characterized NDSS genes of other fungi. Similar sizes have been reported for other NDSS genes responsible for production of intra- and extracellular siderophores. However, the translated NRPS gene of *O. mucida* (Oudmuc1_1435297) was larger than the sizes recorded for the NDSS genes of all the other members of the Physalacriaceae and the characterized NDSS genes from the other fungi.

The number of introns identified in this study compared favorably with those reported for other NDSS genes. The NDSS gene, *FSO1,* in *Om. olearius* has 48 introns (Welzel et al. 2005). The percentage of the translated NDSS genes that were covered by the target sequences (query covers) reported by Le Govic et al. (2018) for NDSS of *S. apiospermum* against the NDSS of *As. fumigatus* Af293 were comparable to those reported herein. The lowest query covers were recorded for the translated NDSS genes of *A. novae-zelandiae* (Armnov1_1625296) and *O. mucida* (Oudmuc1_1435297) in comparison with the characterized NDSS genes of the other fungi.

Our results indicate that the NDSS genes identified in the studied Physalacriaceae genomes encode siderophore synthetases. The $(A\text{-}T\text{-}C)_3(T\text{-}C)_2$ domain architecture, observed in this study, has been previously reported for NDSSs from *As. fumigatus*, *As. nidulans*, *E. festucae*, *F. sacchari, Om. olearius*, and *U. maydis* (Johnson et al. 2013; Munawar et al. 2013; Schwecke et al. 2006; Welzel et al. 2005). These proteins synthesize the hydroxamate-type siderophores, ferricrocin (Schrettl et al. 2008; Wallner et al. 2009), ferricrocin (Eisendle et al. 2003), epichloënin A (Johnson et al. 2013; Koulman et al. 2012), ferrirhodin (Munawar et al. 2013), ferrichrome A (Welzel et al. 2005), and ferrichrome A (Yuan et al. 2001), respectively. All genes encoding these proteins, except the gene encoding AAX49356.1 of *Om. olearius*, were orthologous to the genes for NDSSs predicted in the studied Physalacriaceae.

Results from this study provide some insights into the characteristics of the putative NDSSs of the studied Physalacriaceae. The variations in products biosynthesized by known NDSSs, irrespective of similarities in domain architectures, demonstrate that NRPSs with the same/similar architectures can synthesize different siderophores (Schwecke et al. 2006). Likewise, NDSS genes which differ in their domain architectures have been found to synthesize homologous products (Schwecke et al. 2006). Hence, based on domain architectures, similarity of the products of the presently predicted NDSSs to that reported for the orthologous NDSSs which synthesize the characterized siderophores in other fungi cannot be fully established. It is also unclear, based on the domain architectures in comparison to characterized NDSSs, if the siderophores produced by the NDSS genes of members of the Physalacriaceae are intracellular, extracellular, or both.

A-domain phylogeny, Stachelhaus sequences, and substrate specificity

Phylogeny of the A-domains of NDSSs in the *Armillaria* and *Desarmillaria* species showed that the domains are highly conserved. The phylogenetic analyses also placed the A-domains into three well supported orthologous groups, which have been designated A1, A2 and A3. The Stachelhaus codes and the associated predicted substrate specificities of the A-domains were similar to the observations made using the phylogenetic analyses. The codes DPMMWMAINK, DVLFIITIIK, DVQHTITVVK, and DVQHTITIVK have been previously reported in other NDSSs (Schwecke et al. 2006).

The A1 domain code, DPMMWMAINK, has previously been predicted to activate serine (Schwecke et al. 2006). However, NRPSPredictor2 failed to allow for the prediction of a

substrate specificity for the A1 domains bearing DPMMWMAINK code in the NDSSs identified in this study except for those of *D. tabescens* and *C. torrendii*. The predicted candidate substrates of the A1 domains of these species were three proteinogenic amino acids with hydrophobic side chains (val, leucine (leu), and iso), and two non-proteinogenic amino acids (L-alpha-aminobutyric acid (abu) and isovaline (iva)).

The A2-domain codes DVLFIITIIK, DVQHTITIVK, and DVQHTITVVK have previously been predicted to activate glycine (Schwecke et al. 2006). However, the results from our study suggest that DVLFIITIIK activates proline (pro) or leu, DVQHTITIVK activates pro, and DVQHTITVVK activates hydrophobic-aliphatic amino acids in general.

The A3-domain codes found in the members of the Physalacriaceae differed from the A3-domain codes previously reported for other characterized NDSSs in *As. fumigatus, As. nudilans, E. festucae, Om. olearius,* and *U. maydis* (Johnson et al. 2007; Schwecke et al. 2006; Welzel et al. 2005; Winterberg et al. 2010). The A3 domains of the NRPSs of these species activate N^5-hydroxy-L-ornithine (L-AHO), N^5-*trans*-anhydromevalonyl-N^5-hydroxyornithine (*trans*-AMHO), *N*5-*trans*-(α-methyl)-glutaconyl-N^5-hydroxy-L-ornithine (L-MGHO), and N^5-*trans*-(α-methyl)-glutaconyl-N^5-hydroxy-L-ornithine (L-MGHO), respectively (Schwecke et al. 2006; Welzel et al. 2005; Winterberg et al. 2010). It is noteworthy that L-N^5-ornithine monooxygenases have been found to be located within the clusters bearing the characterized NDSSs in the other fungi (Le Govic et al. 2018; Schwecke et al. 2006). No other gene in the characterized NDSS gene clusters in the genomes of the other fungi has been associated with an enzyme linked to the other A-domains of the NRPSs encoded by the respective NRPS genes.

Inaccuracy of NRPS A-domain substrate predictions of various tools including NRPSPredictor2 has previously been reviewed in Vassaux et al. (2019). Nonetheless, we have demonstrated that the A1-A3 domains of the NDSSs predicted in the genomes of the studied *Armillaria* spp. and other members of the Physalacriaceae may also differ in terms of their substrate specificity compared to characterized NDSSs in other fungi.

Siderophore biosynthesis and mycelia growth of selected strains of *Armillaria* spp.

In vitro siderophore biosynthesis was observed in the studied *Armillaria* spp., irrespective of their lifestyle. Change from blue to reddish-orange, orange, purplish-red, and purple correspond to production of monohydroxamate, trihydroxamate, catecholate, and catecholate siderophores respectively, at neutral pH of CAS-assay medium/solution (Arora and Verma 2017; Milagres et al. 1999). Our results show that the *Armillaria* strains included in this study produce both hydroxamate and catecholate siderophores. These results concur with earlier studies in which co-production of different types of siderophores in vitro has been reported for various organisms (Kügler et al. 2020; Maglangit et al. 2019; Wang et al. 2021). To the best of our knowledge, the production of siderophores by strains of *Armillaria* spp. is first to be demonstrated in the present study. Our results serve as preliminary evidence that the NDSS clusters in *Armillaria* spp. are potentially functional and may biosynthesize siderophores. This is important as it has been established by Wiemann et al. (2013) that the mere existence of a SMGC (remnants) in the genomes of organisms such as *Fusarium* spp. does not necessarily translate to production of the associated secondary metabolites.

Different color changes correspond to different nature of siderophores while different color intensities suggest production of different concentration of siderophores (Milagres et al. 1999). In the present study, interspecific variation in siderophore biosynthesis was observed both in

terms of nature and concentration irrespective of the assay used and the lifestyle of the *Armillaria* spp. Inter-specific variation in siderophore biosynthesis has also been reported for *Trichoderma* spp. (Chen et al. 2019). Biosynthesis of different nature and concentration of siderophores were also recorded depending on whether the universal and modified CAS assays were used. To the best of our knowledge, the presently observed differences in siderophore biosynthesis between these two assays has not been previously reported. The CAS agar contained casamino acids while MYA contained malt and yeast extracts. We propose that the observed variations in siderophore biosynthesis in the respective assays may be due to different substrates used by the presently reported NDSS and the suspected NRPS-independent siderophore synthetases in the genomes of *Armillaria* spp. Substrate specificity assays combined with gene modifications and siderophore extraction and characterization will be required to assess this assertion.

Siderophore biosynthesis of *Armillaria* spp. in this study corroborates previous reports of siderophore biosynthesis by various basidiomycetes (Brandenburger et al. 2017; Milagres et al. 1999; Narh Mensah et al. 2018; Welzel et al. 2005). The clear zones at the mycelia margins of some basidiomycetes species cultured on CAS agar reported by Narh Mensah et al. (2018) was, however, not observed in the present study. In *C. subvermispora*, the NDSS, CsNPS2, catalyzes biosynthesis of the trimeric hydroxamate siderophore, basidioferrin (Brandenburger et al. 2017). The NDSS cluster in *Om. olearius*, which contains the orthologous NDSS, FSO1, catalyzes biosynthesis of the hydroxamate siderophore, ferrichrome A (Welzel et al. 2005).

The various strains of *Armillaria* spp. presently studied also showed differential growth rates on CAS. Variation in growth on the respective media was earlier reported for various basidiomycetes and other fungi, as well as gram-positive bacteria due to the toxicity of HDTMA and the sensitivity of the organisms to the HDTMA contained in CAS media (Schwyn and Neilands 1987). As such, the *Armillaria* strains may vary in their response to HDTMA resulting in the different growth rates. It would be interesting to investigate what drives the apparent differential response to HDTMA by *Armillaria* spp.

Conclusions

There is currently a large knowledge gap about secondary metabolism in Ascomycota and Basidiomycota. This study has contributed to bridging this knowledge gap in Basidiomycota from the genomic and biological perspective. We have demonstrated that *Armillaria* spp. generally contain one highly conserved, potentially functional NRPS-dependent siderophore synthetase gene cluster although some interspecific variation in the biosynthetic products of these clusters is expected. The study has also revealed that the identified NRPS-dependent siderophore synthetase gene clusters in the genomes of *Desarmillaria* spp. and the closely related *G. necrorhizus* are more syntenic to those of *Armillaria* spp. than to the other Physalacriaceae species. Additionally, the products of these NRPS-dependent siderophore synthetases and their clusters may be structurally and functionally different (in terms of affinity for ferric iron) from those of the characterized NRPS-dependent siderophore synthetase clusters in other fungal species. Inter-specific variation in siderophore biosynthesis in *Armillaria* spp. was also recorded. Molecular, biochemical, and biological characterization such as gene deletion/mutations, substrate specificity assays, proteomics, metabolomics, and co-culturing will be required to fully characterize the genes in these predicted clusters. Such studies will also be required to determine the function and relevance of the genes in the clusters, investigate the biological roles of the predicted introns in the NRPS-dependent siderophore synthetase genes, determine the biosynthetic model/overall biosynthesis pathway of the

clusters, characterize the products of the clusters, determine the ability of other organisms to utilize the products of the clusters as xenosiderophores, and to elucidate the role of the products in pathogenicity/virulence as well as other biological functions of these products if any. This is the first report of siderophore biosynthesis by strains of *Armillaria* spp.

Acknowledgements

We are grateful to Dr. László G. Nagy and his team at Biological Research Centre, Synthetic and Systems Biology Unit, 6726 Szeged, Hungary for granting us permission to use the genome and RNA sequence data of *A. borealis* strain FPL87.14, *A. fumosa* strain CBS 122221, *A. mellea* strain ELDO17, *A. nabsnona* strain CMW6904, *A. novae-zelandiae* strain 2840, *D. ectypa* strain FPL83.16 and *D. tabescens* strain CCBAS 213. We also thank all the funding bodies for financial assistance to carry out this work.

Funding

Funding was received from the University of Pretoria, the South African Department of Science and Innovation (DSI)-National Research Foundation (NRF) Centre of Excellence in Plant Health Biotechnology (CPHB, previously the CTHB), the DSI – NRF South African Research Chairs Initiative (SARChI) in Fungal Genomics (Grant number: 98353), and the Tree Protection Cooperative Program (TPCP). The grant holders acknowledge that opinions, findings, and conclusions or recommendations expressed in this publication are that of the authors, and that the funding bodies accept no liability whatsoever in this regard.

Contributions

All authors contributed to the study conception, methodology, analyses of data, and interpretation of the results. DLNM conducted the experiments and a significant part of the data analyses. BDW and MPAC provided supervision and resources. The first draft of the manuscript was written by DLNM and she prepared the figures. All authors commented on previous versions of the manuscript. All authors read and approved the final manuscript.

Conflict of interest

The authors declare that they have no known competing financial interests or personal relationships that could have appeared to influence the work reported in this paper.

Data availability

Publicly available genome and RNA sequences were analyzed in this study. These data can be found at https://mycocosm.jgi.doe.gov/mycocosm/species-tree/tree;05h0Ue?organism=physalacriaceae. Unpublished genome and RNA sequence data obtained from JGI were used with permission from Dr. László G. Nagy. Data of bioassays are presented in this manuscript and can be assessed in the manuscript.

References

Agger S, Lopez-Gallego F, Schmidt-Dannert C (2009) Diversity of sesquiterpene synthases in the basidiomycete *Coprinus cinereus*. Mol Microbiol 72(5):1181–1195

Alexander DB, Zuberer DA (1991) Use of chrome azurol S reagents to evaluate siderophore production by rhizosphere bacteria. Biol Fertil Soils 12(1):39–45

Amin SA, Green DH, Hart MC, Küpper FC, Sunda WG, Carrano CJ (2009) Photolysis of iron–siderophore chelates promotes bacterial–algal mutualism. Proc Natl Acad Sci U S A 106(40):17071–17076

Amnuaykanjanasin A, Punya J, Paungmoung P, Rungrod A, Tachaleat A, Pongpattanakitshote S, Cheevadhanarak S, Tanticharoen M (2005) Diversity of type I polyketide synthase genes in the wood-decay fungus *Xylaria* sp. Bcc 1067. FEMS Microbiol Lett 251(1):125–136

Arora NK, Verma M (2017) Modified microplate method for rapid and efficient estimation of siderophore produced by bacteria. 3 Biotech 7(6):381

Audenaert K, Pattery T, Cornelis P, Höfte M (2002) Induction of systemic resistance to *Botrytis cinerea* in tomato by *Pseudomonas aeruginosa* 7NSK2: Role of salicylic acid, pyochelin, and pyocyanin. Mol Plant-Microbe Interact 15(11):1147–1156

Bachmann BO, Ravel J (2009) Methods for *in silico* prediction of microbial polyketide and nonribosomal peptide biosynthetic pathways from DNA sequence data. In: Hopwood DA (ed) Methods in Enzymology. Academic Press, pp 181–217

Baumgartner K, Rizzo DM (2002) Spread of *Armillaria* root disease in a California vineyard. Am J Enol Vitic 53(3):197–203

Blin K, Pascal Andreu V, de Los Santos ELC, Del Carratore F, Lee SY, Medema MH, Weber T (2019a) The antiSMASH database version 2: A comprehensive resource on secondary metabolite biosynthetic gene clusters. Nucleic Acids Res 47(D1):D625–d630

Blin K, Shaw S, Steinke K, Villebro R, Ziemert N, Lee SY, Medema MH, Weber T (2019b) antiSMASH 5.0: Updates to the secondary metabolite genome mining pipeline. Nucleic Acids Res 47(W1):W81–W87

Brandenburger E, Gressler M, Leonhardt R, Lackner G, Habel A, Hertweck C, Brock M, Hoffmeister D (2017) A highly conserved basidiomycete peptide synthetase produces a trimeric hydroxamate siderophore. Appl Environ Microbiol 83(21):e01478-e11417

Butaitė E, Baumgartner M, Wyder S, Kümmerli R (2017) Siderophore cheating and cheating resistance shape competition for iron in soil and freshwater *Pseudomonas* communities. Nat Commun 8(1):414

Carrano CJ, Jordan M, Drechsel H, Schmid DG, Winkelmann G (2001) Heterobactins: A new class of siderophores from *Rhodococcus erythropolis* IGTS8 containing both hydroxamate and catecholate donor groups. Biometals 14(2):119–125

Chen L, Bóka B, Kedves O, Nagy VD, Szűcs A, Champramary S, Roszik R, Patocskai Z, Münsterkötter M, Huynh T (2019) Towards the biological control of devastating forest pathogens from the genus *Armillaria*. Forests 10(11):1013

Coetzee MPA, Wingfield BD, Roux J, Crous PW, Denman S, Wingfield MJ (2003) Discovery of two northern hemisphere *Armillaria* species on proteaceae in South Africa. Plant Pathol 52(5):604–612

Coetzee MPA, Wingfield BD, Bloomer P, Wingfield MJ (2005) Phylogenetic analyses of DNA sequences reveal speciespartitions amongst isolates of Armillaria from Africa. Mycol Res 109(11):1223–1234

Devireddy LR, Hart DO, Goetz DH, Green MR (2010) A mammalian siderophore synthesized by an enzyme with a bacterial homolog involved in Enterobactin production. Cell 141(6):1006–1017

Eisendle M, Oberegger H, Zadra I, Haas H (2003) The siderophore system is essential for viability of *Aspergillus nidulans*: Functional analysis of two genes encoding L-ornithine N^5-monooxygenase (*sidA*) and a non-ribosomal peptide synthetase (*sidC*). Mol Microbiol 49(2):359–375

Elías-Román RD, Medel-Ortiz R, Alvarado-Rosales D, Hanna JW, Ross-Davis AL, Kim MS, Klopfenstein NB (2018) *Armillaria mexicana*, a newly described species from Mexico. Mycologia 110(2):347–360

Engels B, Heinig U, Grothe T, Stadler M, Jennewein S (2011) Cloning and characterization of an *Armillaria gallica* cDNA encoding protoilludene synthase, which catalyzes the first committed step in the synthesis of antimicrobial melleolides. J Biol Chem 286(9):6871–6878

Evdokias G, Semper C, Mora-Ochomogo M, Di Falco M, Nguyen TTM, Savchenko A, Tsang A, Benoit-Gelber I (2021) Identification of a novel biosynthetic gene cluster in *Aspergillus niger* using comparative genomics. J Fungi 7(5):374

Floudas D, Held BW, Riley R, Nagy LG, Koehler G, Ransdell AS, Younus H, Chow J, Chiniquy J, Lipzen A et al (2015) Evolution of novel wood decay mechanisms in agaricales revealed by the genome sequences of *Fistulina hepatica* and *Cylindrobasidium torrendii*. Fungal Genet Biol 76:78–92

Gaitatzis N, Kunze B, Müller R (2001) *In vitro* reconstitution of the myxochelin biosynthetic machinery of *Stigmatella aurantiaca* sg a15: Biochemical characterization of a reductive release mechanism from nonribosomal peptide synthetases. Proc Natl Acad Sci U S A 98(20):11136–11141

Goering AW, McClure RA, Doroghazi JR, Albright JC, Haverland NA, Zhang Y, Ju K-S, Thomson RJ, Metcalf WW, Kelleher NL (2016) Metabologenomics: Correlation of microbial gene clusters with metabolites drives discovery of a nonribosomal peptide with an unusual amino acid monomer. ACS Cent Sci 2(2):99–108

Gu S, Wei Z, Shao Z, Friman V-P, Cao K, Yang T, Kramer J, Wang X, Li M, Mei X et al (2020) Competition for iron drives phytopathogen control by natural rhizosphere microbiomes. Nat Microbiol 5(8):1002–1010

Gunde-Cimerman N, Cimerman A (1995) *Pleurotus* fruiting bodies contain the inhibitor of 3-hydroxy-3-methylglutaryl-coenzyme a reductase—lovastatin. Exp Mycol 19(1):1–6

Haas H, Eisendle M, Turgeon BG (2008) Siderophores in fungal physiology and virulence. Annu Rev Phytopathol 46(1):149–187

Iftime D, Kulik A, Härtner T, Rohrer S, Niedermeyer THJ, Stegmann E, Weber T, Wohlleben W (2016) Identification and activation of novel biosynthetic gene clusters by genome mining in the kirromycin producer *Streptomyces collinus* tü 365. J Ind Microbiol Biotechnol 43(2):277–291

Johnson LJ, Koulman A, Christensen M, Lane GA, Fraser K, Forester N, Johnson RD, Bryan GT, Rasmussen S (2013) An extracellular siderophore is required to maintain the mutualistic interaction of *Epichloë festucae* with *Lolium perenne*. PLOS Pathog 9(5):e1003332

Johnson LJ, Steringa M, Koulman A, Christensen M, Johnson RD, Voisey CR, Bryan G, Lamont I, Rasmussen S (2007) Biosynthesis of an extracellular siderophore is essential for maintenance of mutualistic endophyte-grass symbioses. In: Popay AJ, Thom ER, (eds) 6th International Symposium on Fungal Endophytes of Grasses. Dunedin, New Zealand: New Zealand Grasslands Association. pp 177–179

Kadi N, Challis GL (2009) Siderophore biosynthesis: a substrate specificity assay for nonribosomal peptide synthetase-independent siderophore synthetases involving trapping of acyl-adenylate intermediates with hydroxylamine. Methods in enzymology. Academic Press, pp 431–457

Koch RA, Wilson AW, Séné O, Henkel TW, Aime MC (2017) Resolved phylogeny and biogeography of the root pathogen *Armillaria* and its gasteroid relative, *Guyanagaster*. BMC Evol Biol 17(1):33

Koch RA, Yoon GM, Aryal UK, Lail K, Amirebrahimi M, LaButti K, Lipzen A, Riley R, Barry K, Henrissat B et al (2021) Symbiotic nitrogen fixation in the reproductive structures of a basidiomycete fungus. Curr Biol 31(17):3905-3914.e3906

König S, Romp E, Krauth V, Rühl M, Dörfer M, Liening S, Hofmann B, Häfner A-K, Steinhilber D, Karas M et al (2019) Melleolides from honey mushroom inhibit 5-lipoxygenase via cys159. Cell Chem Biol 26(1):60-70.e64

Koulman A, Lee TV, Fraser K, Johnson L, Arcus V, Lott JS, Rasmussen S, Lane G (2012) Identification of extracellular siderophores and a related peptide from the endophytic fungus *Epichloë festucae* in culture and endophyte-infected *Lolium perenne*. Phytochemistry 75:128–139

Kügler S, Cooper RE, Boessneck J, Küsel K, Wichard T (2020) Rhizobactin b is the preferred siderophore by a novel *Pseudomonas* isolate to obtain iron from dissolved organic matter in peatlands. Biometals 33(6):415–433

Kuo T-H, Yang C-T, Chang H-Y, Hsueh Y-P, Hsu C-C (2020) Nematode-trapping fungi produce diverse metabolites during predator–prey interaction. Metabolites 10(3):117

Kurth C, Kage H, Nett M (2016) Siderophores as molecular tools in medical and environmental applications. Org Biomol Chem 14(35):8212–8227

Le Govic Y, Papon N, Le Gal S, Bouchara JP, Vandeputte P (2019) Non-ribosomal peptide synthetase gene clusters in the human pathogenic fungus scedosporium apiospermum. Front Microbiol 10(2062):2062

Le Govic Y, Papon N, Le Gal S, Lelièvre B, Bouchara J-P, Vandeputte P (2018) Genomic organization and expression of iron metabolism genes in the emerging pathogenic mold *Scedosporium apiospermum*. Front Microbiol 9:827

Legrand P, Ghahari S, Guillaumin J-J (1996) Occurrence of genets of Armillaria spp. in four mountain forests in Central France: The colonization strategy of *Armillaria ostoyae*. New Phytol 133(2):321–332

Macheleidt J, Mattern DJ, Fischer J, Netzker T, Weber J, Schroeckh V, Valiante V, Brakhage AA (2016) Regulation and role of fungal secondary metabolites. Annu Rev Genet 50(1):371–392

Maglangit F, Tong MH, Jaspars M, Kyeremeh K, Deng H (2019) Legonoxamines A-B, two new hydroxamate siderophores from the soil bacterium, *Streptomyces* sp. Ma37. Tetrahedron Lett 60(1):75–79

May JJ, Wendrich TM, Marahiel MA (2001) The dhb operon of *Bacillus subtilis* encodes the biosynthetic template for the catecholic siderophore 2,3-dihydroxybenzoate-glycine-threonine trimeric ester bacillibactin. J Biol Chem 276(10):7209–7217

Medema MH, Blin K, Cimermancic P, de Jager V, Zakrzewski P, Fischbach MA, Weber T, Takano E, Breitling R (2011) antiSMASH: Rapid identification, annotation and analysis of secondary metabolite biosynthesis gene clusters in bacterial and fungal genome sequences. Nucleic Acids Res 39:W339–W346

Medema MH, Kottmann R, Yilmaz P, Cummings M, Biggins JB, Blin K, de Bruijn I, Chooi YH, Claesen J, Coates RC et al (2015) Minimum information about a biosynthetic gene cluster. Nat Chem Biol 11(9):625–631

Mesanza N, Patten CL, Iturritxa E (2017) Distribution and characterization of *Armillaria* complex in Atlantic forest ecosystems of Spain. Forests 8(7):235

Milagres AMF, Machuca A, Napoleão D (1999) Detection of siderophore production from several fungi and bacteria by a modification of chrome azurol S (CAS) agar plate assay. J Microbiol Methods 37(1):1–6

Mukherjee PK, Hurley JF, Taylor JT, Puckhaber L, Lehner S, Druzhinina I, Schumacher R, Kenerley CM (2018) Ferricrocin, the intracellular siderophore of *Trichoderma virens*, is involved in growth, conidiation, gliotoxin biosynthesis and induction of systemic resistance in maize. Biochem Biophys Res Commun 505(2):606–611

Munawar A, Marshall JW, Cox RJ, Bailey AM, Lazarus CM (2013) Isolation and characterisation of a ferrirhodin synthetase gene from the sugarcane pathogen *Fusarium sacchari*. ChemBioChem 14(3):388–394

Narh Mensah DL, Duponnois R, Bourillon J, Gressent F, Prin Y (2018) Biochemical characterization and efficacy of *Pleurotus*, *Lentinus* and *Ganoderma* parent and hybrid mushroom strains as biofertilizers of attapulgite for wheat and tomato growth. Biocatal Agric Biotechnol 16:63–72

Oide S, Moeder W, Krasnoff S, Gibson D, Haas H, Yoshioka K, Turgeon BG (2006) *Nps6*, encoding a nonribosomal peptide synthetase involved in siderophore-mediated iron metabolism, is a conserved virulence determinant of plant pathogenic ascomycetes. Plant Cell 18(10):2836–2853

Paauw A, Leverstein-van Hall MA, van Kessel KP, Verhoef J, Fluit AC (2009) Yersiniabactin reduces the respiratory oxidative stress response of innate immune cells. PLoS ONE 4(12):e8240

Patzer SI, Braun V (2010) Gene cluster involved in the biosynthesis of griseobactin, a catechol-peptide siderophore of *Streptomyces* sp. Atcc 700974. J Bacteriol 192(2):426–435

Prospero S, Holdenrieder O, Rigling D (2004) Comparison of the virulence of *Armillaria cepistipes* and *Armillaria ostoyae* on four Norway spruce provenances. Forest Pathol 34(1):1–14

Pusztahelyi T, Holb I, Pócsi I (2015) Secondary metabolites in fungus-plant interactions. Front Plant Sci 6:573

Rausch C, Weber T, Kohlbacher O, Wohlleben W, Huson DH (2005) Specificity prediction of adenylation domains in nonribosomal peptide synthetases (NRPS) using Transductive Support Vector Machines (TSVMs). Nucleic Acids Res 33(18):5799–5808

Röttig M, Medema MH, Blin K, Weber T, Rausch C, Kohlbacher O (2011) NRPSpredictor2—a web server for predicting nrps adenylation domain specificity. Nucleic Acids Res 39:W362–W367

Ruiz-Dueñas FJ, Barrasa JM, Sánchez-García M, Camarero S, Miyauchi S, Serrano A, Linde D, Babiker R, Drula E, Ayuso-Fernández I et al (2021) Genomic analysis enlightens Agaricales lifestyle evolution and increasing peroxidase diversity. Mol Biol Evol 38(4):1428–1446

Salwan R, Sharma V (2020) Molecular and biotechnological aspects of secondary metabolites in Actinobacteria. Microbiol Res 231:126374

Sayari M, van der Nest MA, Steenkamp ET, Soal NC, Wilken PM, Wingfield BD (2019) Distribution and evolution of nonribosomal peptide synthetase gene clusters in the Ceratocystidaceae. Genes 10(5):328

Schrettl M, Bignell E, Kragl C, Sabiha Y, Loss O, Eisendle M, Wallner A, Arst HN Jr, Haynes K, Haas H (2007) Distinct roles for intra- and extracellular siderophores during *Aspergillus fumigatus* infection. PLoS Pathog 3(9):1195–1207

Schrettl M, Kim HS, Eisendle M, Kragl C, Nierman WC, Heinekamp T, Werner ER, Jacobsen I, Illmer P, Yi H et al (2008) SreA-mediated iron regulation in *Aspergillus fumigatus*. Mol Microbiol 70(1):27–43

Schwecke T, Göttling K, Durek P, Dueñas I, Käufer NF, Zock-Emmenthal S, Staub E, Neuhof T, Dieckmann R, von Döhren H (2006) Nonribosomal peptide synthesis in *Schizosaccharomyces pombe* and the architectures of ferrichrome-type siderophore synthetases in fungi. ChemBioChem 7(4):612–622

Schwyn B, Neilands JB (1987) Universal chemical assay for the detection and determination of siderophores. Anal Biochem 160(1):47–56

Sipos G, Prasanna AN, Walter MC, O'Connor E, Bálint B, Krizsán K, Kiss B, Hess J, Varga T, Slot J et al (2017) Genome expansion and lineage-specific genetic innovations in the forest pathogenic fungi *Armillaria*. Nat Ecol Evol 1(12):1931–1941

Stachelhaus T, Mootz HD, Marahiel MA (1999) The specificity-conferring code of adenylation domains in nonribosomal peptide synthetases. Chem Biol 6(8):493–505

Stecher G, Tamura K, Kumar S (2020) Molecular evolutionary genetics analysis (MEGA) across computing platforms. Mol Biol Evol 37(4):1237–1239

Stubbendieck RM, Straight PD (2016) Multifaceted interfaces of bacterial competition. J Bacteriol 198(16):2145–2155

Sullivan MJ, Petty NK, Beatson SA (2011) Easyfig: A genome comparison visualizer. Bioinformatics 27(7):1009–1010

Taguchi F, Suzuki T, Inagaki Y, Toyoda K, Shiraishi T, Ichinose Y (2010) The siderophore pyoverdine of *Pseudomonas syringae* pv. Tabaci 6605 is an intrinsic virulence factor in host tobacco infection. J Bacteriol 192(1):117–126

Tsykun T, Rigling D, Nikolaychuk V, Prospero S (2012) Diversity and ecology of *Armillaria* species in virgin forests in the Ukrainian Carpathians. Mycol Progress 11(2):403–414

Vassaux A, Meunier L, Vandenbol M, Baurain D, Fickers P, Jacques P, Leclère V (2019) Nonribosomal peptides in fungal cell factories: From genome mining to optimized heterologous production. Biotechnol Adv 37(8):107449

Wallner A, Blatzer M, Schrettl M, Sarg B, Lindner H, Haas H (2009) Ferricrocin, a siderophore involved in intra- and transcellular iron distribution in *Aspergillus fumigatus*. Appl Environ Microbiol 75(12):4194–4196

Walsh CT (2008) The chemical versatility of natural-product assembly lines. Acc Chem Res 41(1):4–10

Wang X, Zhang M, Loh B, Leptihn S, Ahmed T, Li B (2021) A novel NRPS cluster, acquired by horizontal gene transfer from algae, regulates siderophore iron metabolism in *Burkholderia seminalis* r456. Int J Biol Macromol 182:838–848

Warwell MV, McDonald GI, Hanna JW, Kim M-S, Lalande BM, Stewart JE, Hudak AT, Klopfenstein NB (2019) *Armillaria altimontana* is associated with healthy western white pine (*Pinus monticola*): potential *in situ* biological control of the Armillaria root disease pathogen, *A* Solidipes. Forests 10(4):294

Welzel K, Eisfeld K, Antelo L, Anke T, Anke H (2005) Characterization of the ferrichrome a biosynthetic gene cluster in the homobasidiomycete *Omphalotus olearius*. FEMS Microbiol Lett 249(1):157–163

Wiemann P, Sieber CMK, von Bargen KW, Studt L, Niehaus E-M, Espino JJ, Huß K, Michielse CB, Albermann S, Wagner D et al (2013) Deciphering the cryptic genome: genome-wide analyses of the rice pathogen *Fusarium fujikuroi* reveal complex regulation of secondary metabolism and novel metabolites. PLOS Pathog 9(6):e1003475

Winterberg B, Uhlmann S, Linne U, Lessing F, Marahiel MA, Eichhorn H, Kahmann R, Schirawski J (2010) Elucidation of the complete ferrichrome a biosynthetic pathway in *Ustilago maydis*. Mol Microbiol 75(5):1260–1271

Yuan WM, Gentil GD, Budde AD, Leong SA (2001) Characterization of the *Ustilago maydis* sid2 gene, encoding a multidomain peptide synthetase in the ferrichrome biosynthetic gene cluster. J Bacteriol 183(13):4040–4051

Zheng D, Zeng Z, Xue B, Deng Y, Sun M, Tang Y-J, Ruan L (2018) *Bacillus thuringiensis* produces the lipopeptide thumolycin to antagonize microbes and nematodes. Microbiol Res 215:22–28